IEEE Access
Multidisciplinary | Rapid Review | Open Access Journal

Received August 20, 2019, accepted August 31, 2019, date of publication September 9, 2019, date of current version September 20, 2019.

Digital Object Identifier 10.1109/ACCESS.2019.2940140

Reset Control for DC–DC Converters: An Experimental Application

UNNIKRISHNAN RAVEENDRAN NAIR[1], RAMON COSTA-CASTELLÓ[1], AND ALFONSO BAÑOS[2]

[1]Institut de Robòtica i Informòtica industrial, Universitat Politècnica de Catalunya, 08034 Barcelona, Spain
[2]Departmento Informática y Sistemas, Universidad de Murcia, 30100 Murcia, Spain

Corresponding author: Unnikrishnan Raveendran Nair (uraveendran@iri.upc.edu)

This work was supported in part by the European Union's Horizon 2020 Research and Innovation Programme under the Marie Skłodowska Curie under Grant 675318 (INCITE), in part by the Spanish State Research Agency through the Mara de Maeztu Seal of Excellence to IRI under Grant MDM-2016-0656, and in part by the Government of Spain under Project DPI2016-79278-C2-1-R, MICAPEM (ref. DPI2015- 69286-C3-2-R, MINECO/FEDER).

ABSTRACT Power converters in grid connected systems are required to have fast response to ensure the stability of the system. The standard PI controllers used in most power converters are capable of fast response but with significant overshoot. In this paper a hybrid control technique for power converter using a reset $PI + CI$ controller is proposed. The $PI + CI$ controller can overcome the limitation of its linear counterpart (PI) and ensure a fast flat response for power converter. The design, stability and cost of feedback analysis for a DC-DC boost converter employing a $PI+CI$ controller is explored in this work. The simulation and experimental results which confirm the fast, flat response will be presented and discussed.

INDEX TERMS Hybrid control, reset systems, energy systems, DC-DC converter, stability.

I. INTRODUCTION

Reset controllers were first introduced by J C Clegg through the Clegg integrators (CI) for servo systems [1]. The CI is a hybrid dynamical system which resets its output to zero when input becomes zero providing improved performance and reduced overshoot. This was followed by many works involving different reset controllers like First Order Reset Elements (FORE) [2]–[6] and more recently $PI + CI$ controllers [7]–[9]. The reset controllers are capable of overcoming limitations of its linear counterparts and provide improved performance [10]. A general background on reset control systems can be obtained from the monograph [11].

The $PI + CI$ controller employs the CI along with a PI controller to improve its performance. The CI on its own is not able to ensure zero steady-state error unless there is an integrator in the plant. The $PI + CI$ uses integrator from PI controller to eliminate steady-state error and CI to achieve improved performance by allowing fast response with reduced overshoot. There has been many works done in the area of $PI+CI$ controllers involving laying out design criteria [8], [9] for different plants and stability analysis of such systems [7], [12], [13]. The application of such controllers in real world applications like pH in-line control [9], bilateral teleoperation [14], solar collector field [15], industrial wafer scanners [16] and control of industrial heat exchangers [17] have been explored.

Power converters in grid connected systems present an interesting field for the application of reset $PI + CI$ controllers. Modern grids are seeing increased penetration of renewable energy sources (RES) leading to an increased number of power converters in grids [18]. Power converter allow controlling power supplied to grid, power conversion (DC↔AC) and matching of voltage levels [19], [20]. The non dispatchable nature of the power from RES has led to addition of electrical storage systems (ESS) in grid to ensure stable operation [21]. Power converters are again needed for grid connection of ESS. The motivation for using $PI + CI$ controllers for power converters stems from the need for these systems to respond to fast changes in load demands while maintaining the system parameters like voltage, frequency etc. within limits prescribed by grid codes. Sudden load changes can result in voltage flickers or tripping of electrical systems due to large frequency and voltage deviation if systems are not designed to respond quickly [22]. Currently most converters employ PI controllers to achieve reference tracking in their control [23]. These PI controllers are tuned to have fast response to sudden reference change arising from load variations, to maintain grid parameters within prescribed limits. Though PI controllers are capable

The associate editor coordinating the review of this manuscript and approving it for publication was Jianyong Yao.

of such fast response they can have significant overshoot in their transient period highlighting a scope for improvement. As such $PI+CI$ reset controller can be a better choice for such systems with its ability of reduced overshoot as demonstrated through [9], [14]–[17]. $PI+CI$ controllers are also capable of producing a fast flat response for first order plants [9]. This is an important attribute of the $PI + CI$ which can be exploited in converter control.

Many control techniques have been used in power converters to obtain improved transient response to step change in reference like, higher order sliding mode controls [24]–[26] and differential flatness theory based [27] control. Nevertheless, these controllers tend to rely on complex formulations for deriving their control law. The PI+CI controller is a simple modification of the PI controller with a simple control law formulation, improved transient performance and capable of guaranteeing a flat response in first order systems. As far as the authors' knowledge goes the use of such control in power converters have not been explored before.

This work proposes the implementation of PI + CI reset controller for a prototype DC-DC boost converter. The proposed work is an extension of [28] where applicability of reset control in DC-DC converters with ideal averaged converter models where studied. The study in [28] do not consider the practical implementation, where there are the unmodelled effects of measurements delays, data acquisition systems and measurement noise. The scope of this work is on analysing and identifying the robustness of the PI+CI controller design in [28] and well posedness of the reset instances under these unmodelled effects. This is assessed through the experimental implementation of the presented control in a prototype DC-DC converter. The scope is also broadened though establishment of formal stability analysis and robustness to: measurement, switching noise and parameter uncertainty.

The rest of the paper is organised as follows. Section II introduces preliminaries like $PI + CI$ controller model, the reset control systems model, stability conditions and converter models employed. Section III shows the controller design for the proposed DC-DC boost converter, stability analysis, robustness under parameter uncertainty and cost of feedback analysis based on describing functions. Section IV presents the implementation and results obtained from lab along with simulation results. Finally, conclusion and scope for future work will be presented in Section V.

II. PRELIMINARIES

A. RESET CONTROLLER

After the seminal works introducing the CI and the FORE, general single-input single-output reset controllers derived from linear and time invariant base system, were introduced in the late 90's (see [11], [29] and references therein). In [5], the CI and the FORE are reformulated using the hybrid inclusions framework of [30], with a resetting law based on a sector condition over their input-ouput pairs. This modelling has been followed in many subsequent works including some generalizations, for example the model given in [31], which will be adopted in this work. A reset controller $\mathcal{R}$ is given by

$$\mathcal{R} = \begin{cases} \dot{\mathbf{x}}_r = \mathbf{A}_r\mathbf{x}_r + \mathbf{B}_r e, & if\,(e, -u_{\mathcal{R}}) \in \mathcal{F} \\ \mathbf{x}_r^+ = \mathbf{A}_\rho\mathbf{x}_r, & if\,(e, -u_{\mathcal{R}}) \in \mathcal{J} \\ -u_{\mathcal{R}} = \mathbf{C}_r\mathbf{x}_r \end{cases} \tag{1}$$

where $\mathbf{x}_r \in \mathbb{R}^{n_r}$, $\mathbf{A}_r, \mathbf{B}_r$ and $\mathbf{C}_r$ are the appropriate system matrices and $-u_{\mathcal{R}}$ is the output of the reset controller employed. $\mathcal{F}, \mathcal{J}$ are the flow and jump sets of the system respectively. In the set defined by $\mathcal{F}$ the controller states flow according to linear differential equation whereas the states undergo a jump at the set $\mathcal{J}$. $\mathbf{x}_r^+$ represents the state of the controller after jump caused by the reset instance. The matrix $\mathbf{A}_\rho$ is the reset matrix which defines the system states after the reset instance. The flow set $\mathcal{F}$ is given by

$$\mathcal{F} = \{(e, -u_{\mathcal{R}}) \in \mathbb{R}^2 | eu_{\mathcal{R}} \leq -\frac{1}{\alpha}u_{\mathcal{R}}^2\} \tag{2}$$

while $\mathcal{J}$ is given by

$$\mathcal{J} = \{(e, -u_{\mathcal{R}}) \in \mathbb{R}^2 | eu_{\mathcal{R}} \geq -\frac{1}{\alpha}u_{\mathcal{R}}^2\} \tag{3}$$

where $\alpha > 0$ is as shown in Fig. 1a The flow and jump sets defined using the above equations can be illustrated in a two dimensional plane as sectors shown in Fig. 1a. The jump condition occurs along the boundary of $\mathcal{F}$ and $\mathcal{J}$ in Fig. 1a [31]. The general reset controller expression in (1) can be used to express all the different reset controllers. For a detailed exposition to the hybrid inclusions framework, including definition of hybrid time and the solution concept for reset systems, the reader is referred to [30].

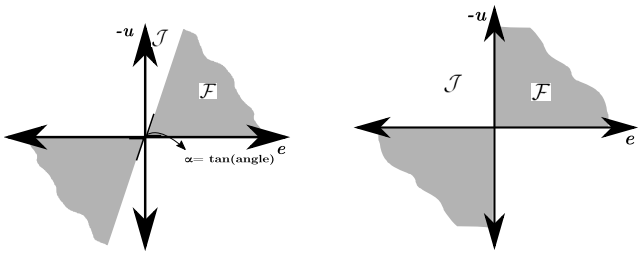

(a) General reset system (b) Clegg integrator(CI)

FIGURE 1. (a), Sector condition for general reset controller. (b), Sector condition for CI with $\alpha \to \infty$.

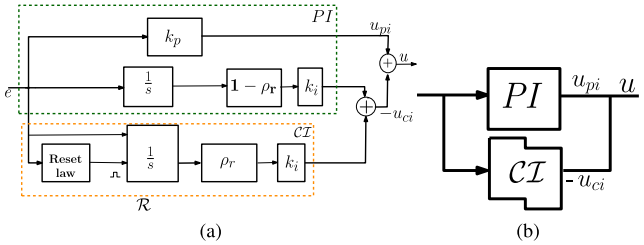

(a) (b)

FIGURE 2. (a), PI+CI controller schematic. (b), An equivalent representation of PI+CI with $\mathcal{R}$ representing CI.

The PI+CI controller considered in this work is obtained by introducing a CI along with the classical PI controller and is schematically represented as in Fig.2. The orange square

region in Fig.2a represents the CI part and the green region represents the PI part. The reset law in CI part is defined by the boundary of $\mathcal{J}$ with $\mathcal{F}$. The term ρ_r is the reset ratio and represents the percentage of the total integral action that gets reset through the CI. For example, if $\rho_r = 0$ it results in a classic PI controller, which will be referred henceforth as PI_{base}, whereas a $\rho_r = 1$ results in P+CI controller. Once the PI_{base} controller has been designed, usually to obtain a fast response, the PI+CI controller acts by removing (or minimizing) the overshoot (and hence the significance of negative output of reset part). The desired design specification (a fast response without overshooting) may be obtained simply by adjusting the parameter ρ_r. As such, in this work, the design problem will be to find a ρ_r value between 0 and 1 which will ensure a flat response and an improved performance over PI controller.

The PI+CI controller [8] can be modelled as in (1) using:

$$\begin{cases} \dot{\mathbf{x}}_r = \mathbf{A}_r\mathbf{x}_r + \mathbf{B}_r e, & if\,(e, -u_{ci}) \in \mathcal{F} \\ \mathbf{x}_r^+ = \mathbf{A}_\rho\mathbf{x}_r, & if\,(e, -u_{ci}) \in \mathcal{J} \\ u = \mathbf{C}_r(\rho_r)\mathbf{x}_r + \mathbf{D}_r e \end{cases} \tag{4}$$

where $\mathbf{x}_r = [x_i\ x_{ci}]^T$ are the states of the controller defined by the integrator (x_i) and CI (x_{ci}) states, and

$$\mathbf{A}_r \triangleq \begin{bmatrix} 0 & 0 \\ 0 & 0 \end{bmatrix}, \quad \mathbf{B}_r \triangleq \begin{bmatrix} 1 \\ 1 \end{bmatrix}, \quad \mathbf{C}_r \triangleq k_i \begin{bmatrix} 1-\rho_r & \rho_r \end{bmatrix}$$
$$\mathbf{D}_r \triangleq k_p, \quad \mathbf{A}_\rho \triangleq \begin{bmatrix} 1 & 0 \\ 0 & 0 \end{bmatrix} \tag{5}$$

Note that the dependence of $\mathbf{C}_r$ on ρ_r has been explicitly shown in (4),(5). The sets $\mathcal{F}$ and $\mathcal{J}$ for the PI+CI controller are defined as in (2, 3), where $\alpha > 0$ typically takes a large value (note that for $\alpha \to \infty$ the CI developed in [5] is recovered and this PI+CI controller is equivalent to that developed in [8], as far as its initial conditions are taken in the set $\mathcal{F}$); $-u_{ci}$, u_{pi} is output of CI, PI part respectively and u the output of PI+CI as shown in Fig. 2b. The resulting $\mathcal{F}$ and $\mathcal{J}$ for PI+CI is represented as in Fig. 1b. Although the PI+CI controller can also be built using a variable ρ_r, see [9], for the purposes of this work ρ_r will be a constant parameter.

B. RESET CONTROL AS A HYBRID DYNAMICAL SYSTEM

The Fig.3 shows a general reset control system employing a $PI + CI$ controller. The reference to the system is represented by the exogenous signal $\mathbf{w}_1$ in Fig.3. It is assumed that $\mathbf{w}_1$ is a Bohl function and is represented as

$$\begin{aligned} \dot{\mathbf{w}}_1 &= \mathbf{A}_1\mathbf{w}_1, \mathbf{w}_1(0) = w_{10} \\ r &= \mathbf{C}_1\mathbf{w}_1 \end{aligned} \tag{6}$$

where $\mathbf{w}_1 \in \mathbb{R}^{n_1}$, $\mathbf{A_1}$ and $\mathbf{C_1}$ are appropriate system matrices. As this work considers a reference tracking problem the disturbance inputs are not considered here. The additive input in the feedback path of Fig.3 represents the measurement noise, n. The plant (P) under consideration is represented in

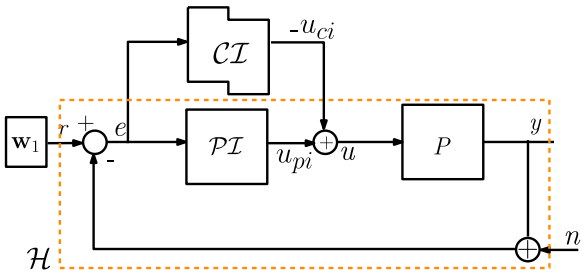

FIGURE 3. Reset control system with a PI+CI controller and exogenous inputs in reference $\mathbf{w_1}$ and measurement noise n.

the state-space form as

$$\begin{aligned} \dot{\mathbf{x}}_p &= \mathbf{A}_p\mathbf{x}_p + \mathbf{B}_p u, \\ y &= \mathbf{C}_p\mathbf{x}_p \end{aligned} \tag{7}$$

where $\mathbf{x}_p \in \mathbb{R}^{n_p}$.

Therefore, using (4), (6), (7) the closed-loop system can be represented by (note that ρ_r is a constant parameter, explicit dependence on is shown)

$$\begin{cases} \dot{\mathbf{x}} = \mathbf{A}(\rho_r)\mathbf{x}, & \mathbf{x} \in \mathcal{F}_\mathcal{C} \\ \mathbf{x}^+ = \mathbf{A}_R\mathbf{x}, & \mathbf{x} \in \mathcal{J}_\mathcal{C} \\ y = \mathbf{C}\mathbf{x} \end{cases} \tag{8}$$

where $\mathbf{x} \in \mathbb{R}^{n_p+2+n_1}$ is the state of closed loop system defined by $[\mathbf{x}_p, \mathbf{x}_r, \mathbf{w}_1]^T$. The matrices $\mathbf{A}$,$\mathbf{C}$, $\mathbf{A}_R$ are defined as

$$\mathbf{A}(\rho_r) \triangleq \begin{bmatrix} \mathbf{A}_p - \mathbf{B}_p\mathbf{D}_r\mathbf{C}_p & \mathbf{B}_p\mathbf{C}_r(\rho_r) & \mathbf{B}_p\mathbf{D}_r\mathbf{C}_1 \\ -\mathbf{B}_r\mathbf{C}_p & \mathbf{A}_r & \mathbf{B}_r\mathbf{C}_1 \\ 0 & 0 & \mathbf{A}_1 \end{bmatrix}$$
$$\mathbf{C} \triangleq (\mathbf{C}_p\ \mathbf{0}_2\ \mathbf{0}_{n1}), \quad \mathbf{A}_R \triangleq diag(\mathbf{I}_{n_p}, \mathbf{A}_\rho, \mathbf{I}_{n_1}) \tag{9}$$

where $\mathbf{I}$ is unit matrix and $\mathbf{0}$ is a zero vector of appropriate order. The set $\mathcal{F}_\mathcal{C}, \mathcal{J}_\mathcal{C}$ is the same as that in (2)-(3) but reformulated as a function of system states given by

$$\mathcal{F}_\mathcal{C} = \{\mathbf{x} \in \mathbb{R}^{n_p+2+n_1} | \mathbf{x}^T\mathcal{M}\mathbf{x} \le 0\} \tag{10}$$

while $\mathcal{J}$ is given by

$$\mathcal{J}_\mathcal{C} = \{\mathbf{x} \in \mathbb{R}^{n_p+2+n_1} | \mathbf{x}^T\mathcal{M}\mathbf{x} \ge 0\} \tag{11}$$

where $\mathcal{M} = \mathbf{C_{\mathcal{F}1}}^T\mathbf{C_{\mathcal{F}2}}\alpha + \mathbf{C_{\mathcal{F}2}}^T\mathbf{C_{\mathcal{F}2}}$ with $\mathbf{C_{\mathcal{F}1}} = [-\mathbf{C}_p\ \mathbf{0}_2\ \mathbf{C}_1]$ and $\mathbf{C_{\mathcal{F}2}} = [\mathbf{0}_{np}\ 0\ -k_i\rho_r\ \mathbf{0}_{n1}]$.

C. ROBUSTNESS AGAINST SENSOR NOISE AND STABILITY

The reset control system (8) trivially satisfies the so-called basic hybrid conditions [30], since the flow and jump maps are continuous and the sets $\mathcal{F}$ and $\mathcal{J}$ are closed. This gives us some desirable properties like robustness against sensor noise, and also robustness in stability, see [30] for detailed results.

In this work, the stability analysis is based on [31]; and according to it, the stability notion is pre-input to state stability (pre-ISS). Since developing an ISS Lyapunov function which can verify the stability of the system can be cumbersome in the case of hybrid systems like reset controllers,

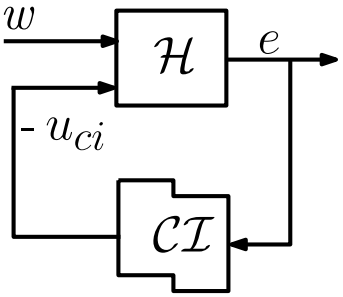

FIGURE 4. Reduced feedback interconnection from Fig.3 of LTI dynamical system ($\mathcal{H}$) and CI controller.

in [31] a nice frequency domain based stability result is proposed.

The Fig.4 shows the feedback interconnection of a dynamical system ($\mathcal{H}$), shown in Fig.3, and the CI controller. The system $\mathcal{H}$ includes all the linear part of the reset control shown in the highlighted region (orange) in Fig.3 with $\mathbf{w}_1 = r$. The system is considered minimal with

$$\mathcal{L}\{e\} = \mathcal{G}_{eu}(s)\mathcal{L}\{u_{ci}\} + \mathcal{G}_{ew}(s)\mathcal{L}\{\mathbf{w}_1\} \tag{12}$$

where $\mathcal{G}_{eu}, \mathcal{G}_{ew}$ are the transfer function of the system between e with u_{ci} and $\mathbf{w}_1$ as inputs respectively.

The stability of system can be guaranteed if it satisfies the following criteria [31]:

1) The system matrix $\mathcal{H}$ is Hurwitz, that is its eigenvalues are strictly in the left half side of complex plane.
2) The transfer function $\mathcal{G}_{eu(s)}$ as in (12) satisfies

$$\frac{1}{\alpha} + Re(\lim_{w\to\infty} \mathcal{G}_{eu(s)}) > 0 \tag{13}$$

and

$$\frac{1}{\alpha} + Re(\mathcal{G}_{eu(s)}) > 0 \quad \forall w \in \mathbb{R} \tag{14}$$

provided matrices $\mathbf{A}_r, \mathbf{C}_r$ in (1,5) is detectable. Satisfying the above criteria will ensure the existence of a pre-ISS Lyapunov function which is smooth with negative derivative between reset instants and decreases in value after a reset instance.

D. DESIGN OF PI+CI CONTROLLER FOR FIRST ORDER PLANTS

Consider a first order plant P given by

$$P(s) = \frac{b_0}{s + a_0}, \tag{15}$$

subjected to an exogenous input $\mathbf{w}_1$ represented by a step signal of amplitude w_{10}. In [9], it is shown that the closed-loop system error can be forced to zero from the first reset by choosing an appropriate value of ρ_r given by [9], [28]

$$\rho_r = 1 - \frac{a_0 w_{10}}{b_0 k_i x_{i,1}} \tag{16}$$

where $x_{i,1}$ is the value of the integrator state x_i at the first reset instance.

The value for ρ_r defined in (16) is dependant on the nature of exogenous signal applied at the input of the system. The above expression is an optimal value of ρ_r for the step input.

E. CONVERTER MODELLING

The proposed PI+CI controller can be used in different DC-DC converter topologies. In this work, it is implemented on a DC-DC boost converter of Fig.5. This converter is interfacing an ESS or renewable source (v_{dc}) to a DC micro-grid and is working in current source mode delivering active power requirements. The inductor l_1 and capacitor c_1 in Fig.5 form the input filter to the DC source, v_{dc}. The inductor l_2 enables the boosting of input voltage to the output (v_{bus}). The resistors r_1 and r_2 are the effective series resistance l_1 and l_2 respectively.

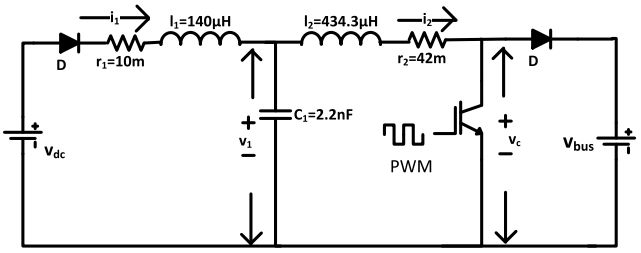

FIGURE 5. DC-DC Boost converter schematic with passive components, switching devices and system state voltages, current.

The averaged large signal model [32] of the converter by neglecting the high frequency switching ripples is used for design purpose. The average voltage across the switch (MOSFET, IGBT) is taken to achieve the same and is defined as $v_c = d' v_{bus}$ where $d' = 1 - d$ with d, the duty ratio of the gate signals. The domain of modelling the converters has been subject to extensive research [23], [32], [33]. The converter model for the system shown in Fig.5 is given by (17) as shown at the bottom of this page.

A variable change is proposed for (17) as shown below

$$V_{m2}(s) \triangleq \frac{V_{dc}(s)}{l_1 c_1 s^2 + r_1 c_1 s + 1} - V_c(s) \tag{18}$$

resulting in a model given by (19) as shown at the bottom of the next page, which will be used for controller design. This variable change is important to ensure that at start up the voltage v_c is same as v_{dc} thereby eliminating large in-rush currents.

$$i_2(s) = \frac{v_{dc}(s) - (c_1 l_1 s^2 + c_1 r_1 s + 1) v_c(s)}{l_1 l_2 c_1 s^3 + c_1(l_1 r_2 + l_2 r_1)s^2 + (c_1 r_1 r_2 + l_1 + l_2)s + (r_1 + r_2)} \tag{17}$$

TABLE 1. Component value used in DC-DC converter.

Component name	Value
l_1	140 μH
l_2	434.3 μH
c_1	2.2nF
r_1	10mΩ
r_2	42mΩ

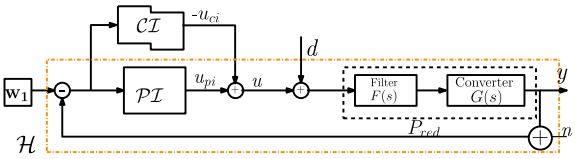

FIGURE 6. The closed-loop representation of the reset control system employed for the boost converter.

III. CONTROLLER DESIGN

The PI+CI control can ensure a fast flat response as shown in the previous section for first order systems. The DC-DC boost converter in Fig.5 though, is a third order system (19) and forcing such a system to have a flat response will be difficult if not impossible with PI+CI controller. Therefore, the original system represented by the converter needs to be reduced so that the system seen by the reset controller is effectively first order. The third-order system presented by the converter is reduced to an effective first order system (P_{red} bounded by the dotted region in Fig.6) using a filter, $F(s)$, designed to have zeros to cancel complex conjugate poles of the converter and poles to cancel the complex conjugate zeros. The Fig.6 is the schematic of the equivalent control system. The converter represented by (19) for the component values shown in Table.1 is represented as

$$G(s) = \frac{i_2(s)}{v_{m2}(s)} = \frac{1742 \cdot (s + 35.70 \pm 1800i)}{(s + 87.1)(s + 38.20 \pm 2070i)} \tag{20}$$

the filter F(s) will therefore be:

$$F(s) = \frac{s + 38.20 \pm 2070i}{s + 35.70 \pm 1800i} \tag{21}$$

ensuring a pole zero compensation resulting in P_{red} given by

$$P_{red}(s) = G(s) \cdot F(s) = \frac{1742}{s + 87.1}. \tag{22}$$

This P_{red} is now considered for the calculation of ρ_r value and as it will be the effective first order system seen by the controller as in (15). The design of the $PI + CI$ is then carried out as follows. First, the PI_{base} parameters k_p and k_i have to be calculated. A base selection of these parameters were carried out using the AMIGO design technique outlined in [34]. The parameters of this base design was then tuned to improve the system performance towards noise entering through plant input as the AMIGO design considers only output noise. This was done since in the DC-DC converter switching noise is introduced at the plant input by converting the control action u in Fig.6 to 20 kHz gate pulses for controlling the IGBTs to achieve the desired output current. A set of PI_{base} parameters were considered and the one with better performance in the real DC-DC converter set up was chosen. As the design of a PI_{base} is not the main objective of this work the detailed analysis of the same is not provided for the sake of brevity.

The k_p and k_i values where calculated to be 0.03316 and 19.39 respectively for a settling time of 0.055s.

The fast settling time though results in a peak overshoot of 28%. The next step is to calculate the value of ρ_r using (16) to obtain the flat response. The $k_i x_{i,1}$ term in (16) is the output of the PI_{base} integrator at the instance of first zero crossing of system error. The value for $k_i x_{i,1}$ was calculated off-line using a model of system controlled by PI_{base} and used in the calculation of ρ_r. This resulted in a value of $\rho_r = 0.4889$. It should be noted that the value of ρ_r obtained here is for the parameter values shown in Table.1.

A. STABILITY ANALYSIS

Stability of the DC-DC boost converter control system is analysed using the results in Section II.D. In the case of $PI + CI$ controller employed for boost converter in this work, the transfer function $\mathcal{G}_{eu}(s)$ is

$$\mathcal{G}_{eu}(s) = \frac{P_{red(s)}}{1 + P_{red(s)} PI(s)} = \frac{1742s}{s^2 + 144.9s + 33780}. \tag{23}$$

The first criteria of the stability condition will be satisfied by designing a stabilizing PI_{base} such that the linear system represented by $\mathcal{H}$ is stable which is also the case here. The transfer function $\mathcal{G}_{eu}(s) \to 0$ as $w \to \infty$ is trivial thereby, satisfying (13). Finally the fulfilment of (14) is explained through Fig.7. This shows the Nyquist plot of the transfer function $\mathcal{G}_{eu}(s)$. The sector condition for CI controller is defined for $\alpha \to \infty$ resulting in the $Re(\mathcal{G}_{eu(s)})$ to lie on the right half side of the complex plane in the Nyquist plot to ensure condition 2. This can be observed in Fig.7. As a result, it is shown that closed-loop system is stable according to Section II.D.

The $PI + CI$ controller used in this work is a hybrid controller and unlike linear systems robustness analysis may not be straightforward. Well-posedness of the reset control systems, as well as robustness to measurement noise and stability easily follow by using the formal methods developed in [30]. The sense of robustness in [30] is related with keeping a desired property, e. g. stability, for arbitrarily small values of for example sensor noise. It is also interesting to analyze if the stability is kept when there exist some parameter uncertainty, which is also a basic issue in control practice.

$$G(s) = \frac{i_2(s)}{v_{m2}(s)} = \frac{c_1 l_1 s^2 + c_1 r_1 s + 1}{l_1 l_2 c_1 s^3 + c_1(l_1 r_2 + l_2 r_1)s^2 + (c_1 r_1 r_2 + l_1 + l_2)s + (r_1 + r_2)} \tag{19}$$

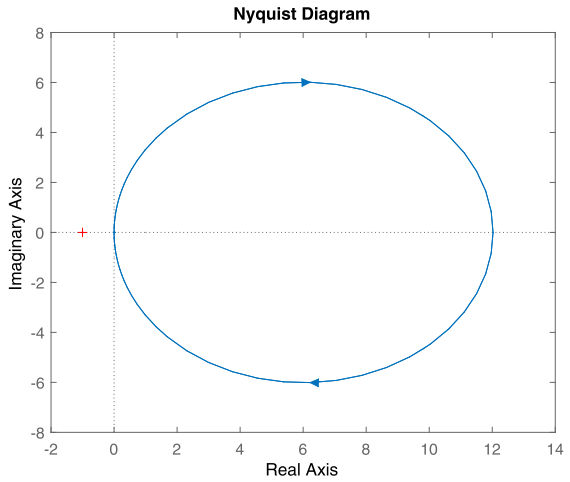

FIGURE 7. Nyquist plot for the transfer function $\mathcal{G}_{eu}(s)$.

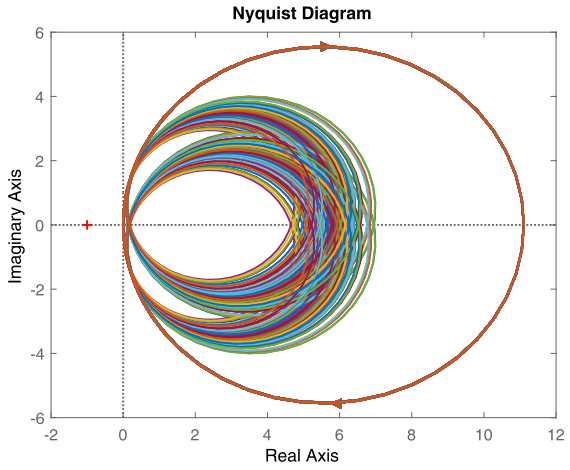

FIGURE 8. Nyquist plots of $\mathcal{G}_{eu}(s)$ for the varying values of the boost converter parameters l_1, l_2, c_1.

An additional advantage of frequency domain analysis it that it easily allows this type of robustness analysis. An analysis is done in the form of controller performance towards parameter uncertainty. The values of inductors and capacitors are usually mentioned within a range defined as a percentage of the nominal value. Under such conditions an exact pole zero cancellation may not be possible and the system may not be exactly first order. The stability of the system under such scenario needs to be ascertained. The uncertainty in the nominal value of the components l_1, l_2 and c_1 considered here is 10%, based on the data-sheet of these components. The stability under uncertainty is ascertained using the results of Section II.D. Satisfying first condition of stability criteria and (13) is trivial. The effect of uncertainty on the condition (14) is highlighted in Fig.8. The plot in Fig.8 is generated using 100 random values of the components l_1, l_2 and c_1 within the uncertainty range. It can be noted despite the uncertainty the Nyquist plots are always positioned on the right half plane of the complex plane ensuring that (14) is always satisfied thereby establishing stability despite uncertainty. The same

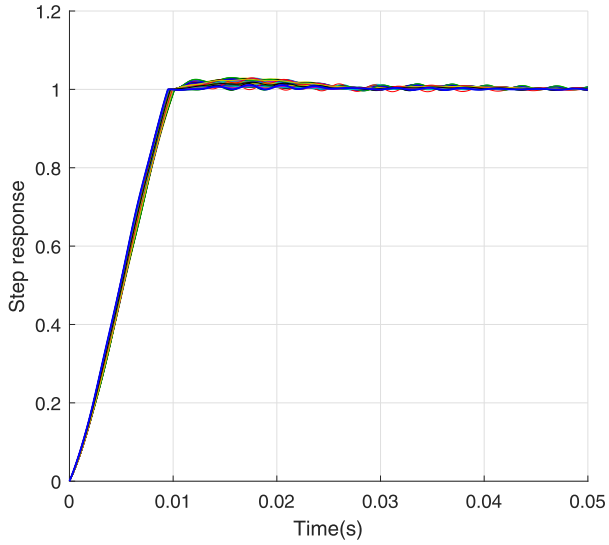

FIGURE 9. Step responses of the designed system for parameter variations in l_1, l_2, c_1 for the designed value of $\rho_r = 0.4889$.

is highlighted in Fig.9. This figure shows the step response of the reset controller based boost converter system taking 100 random samples within the uncertainty range.

B. DESCRIBING FUNCTION ANALYSIS

Having already established closed loop stability of the system in Section II.D the analysis in this section allows a heuristic understanding of the reset system robustness in comparison to linear base system using describing function (DF), which will be otherwise impossible by any other means. Although an approximated analysis, in control practice it gives an adequate characterization of both stability margins and sensor noise effect since the feedback loop has the necessary low-pass property. In this context DF analysis can present itself as a simple tool for a designer to provide an intuition on the robustness of the designed reset controller using well established frequency domain techniques. Whilst DF analysis have been found to fail in some cases it can still be an important tool and its use in non-linear systems have been justified through the works in [35]–[37].

The describing function of a $PI + CI$ is given by [11]

$$PI + CI(\omega) = k_p \frac{j(w\tau_i + \frac{4}{\Pi}\rho_r) + 1}{j\omega\tau_i} \tag{24}$$

where $\tau_i = \frac{kp}{ki}$. The important characteristic of DF of the $PI + CI$ controller is that the function does not depend on the amplitude of the input but solely on the frequency of input. This allows the use of frequency domain analysis tools in analysing the robustness of reset controllers.

The $PI + CI$ controller has been proposed to overcome the inherent limitation of its linear counterparts. Nevertheless it is necessary to investigate whether this is achieved without increasing the cost of feedback (sensitivity to sensor noise) or sensitivity to load disturbance so that its application

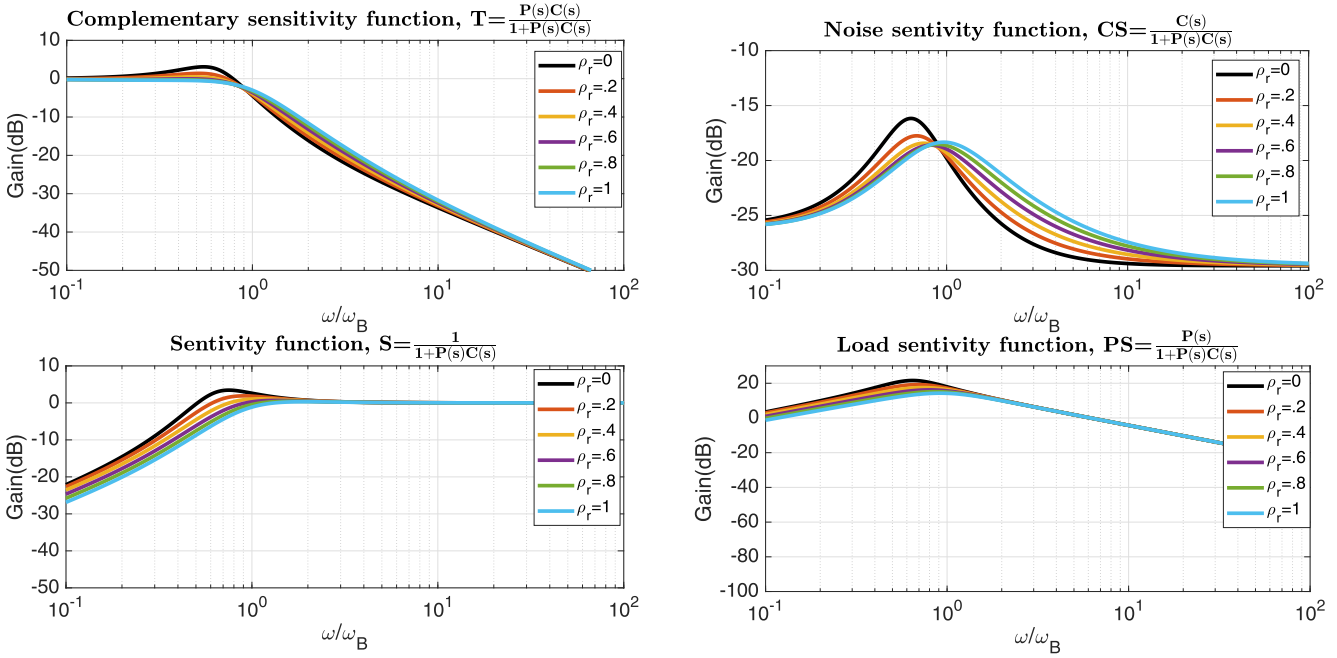

FIGURE 10. Bode plots of the system transfer function including closed loop transfer function (TF), Noise sensitivity Function (CS), sensitivity function (S) and load sensitivity function (PS) plotted for linear base system (ρ_r) = 0 and for different reset ratios.

is justified. An understanding of this can be achieved using the system transfer functions mentioned in [38], which can be constructed using the DF for $PI + CI$ given by (24). The four system transfer functions considered for the same, mentioned in [38], are system complementary sensitivity transfer function (T), sensitivity function (S), noise sensitivity function (CS) and load sensitivity function (PS) given by

$$T(w) = \frac{Y(w)}{w_1(w)} = \frac{PI + CI(w) \cdot P_{red}(jw)}{1 + PI + CI(w) \cdot P_{red}(jw)} \tag{25}$$

$$S(w) = \frac{Y(w)}{N(w)} = \frac{1}{1 + PI + CI(w) \cdot P_{red}(w)} \tag{26}$$

$$CS(w) = \frac{U(w)}{N(w)} = \frac{PI + CI(w)}{1 + PI + CI(w) \cdot P_{red}(w)} \tag{27}$$

$$PS(w) = \frac{U(w)}{N(w)} = \frac{P_{red}(w)}{1 + PI + CI(w) \cdot P_{red}(w)}. \tag{28}$$

The Fig.10 shows Bode plots of eqs. (25) to (28) for varying values of ρ_r. The frequency axis is normalised using the cut-off frequency w_b. It can be observed from Fig.10 that the system reference to output transfer function (T) gains are very similar for the linear ($\rho_r = 0$) and reset system for the entire frequency range. The linear system though will exhibit an higher overshoot compared to reset system based on the plots which is to be expected as the reset action ensures flat response. The closed loop bandwidth remains the same ($w/w_b = 1$) and the reset system performance is very similar to the base system at high frequencies.

The DC/DC converter presented in this work is a system where the noise will enter through the plant input d (Fig.6) in the form of switching noise. The continuous time control input u will be converted to 20 kHz gate pulses for the IGBTs using pulse width modulation (PWM). Therefore an interesting plot to study will be the effect of plant output to noise input d which is given by load sensitivity function (PS). This also allows understanding of load disturbance rejection capability of the plant. It can be seen from Fig.10 that the addition of reset action has actually reduced the sensitivity of the system towards input disturbance. Nevertheless at switching frequency of 20 kHz the gain plots are same showing similar performance. Finally, the effect of measurement (output) noise on the plant performance is studied through the noise sensitivity (CS) and sensitivity (S) functions.The linear base system still exhibits a higher sensitivity in comparison to the reset systems. It should also be noted that in all the above functions higher the reset ratio lesser is the sensitivity of the function. Therefore a general consensus that can be drawn from here is that the reset action does improve the system performance by producing a fast flat response and provides a marginal improvement in system robustness observed by reduced gains in the sensitivity functions. This is still a heuristic understanding and may not be truly reflective of the actual system performance. The real impact of the reset system will be discussed in the next section where results from an actual converter system subjected to measurement and switching noises will be presented.

IV. IMPLEMENTATION AND RESULTS

A. SIMULATION RESULTS

The improvement that can be achieved with the PI+CI control is demonstrated through simulation first. The simulations were done in Matlab-Simulink. The Fig.11 shows reference tracking performance of the plant controlled by the PI_{base} and

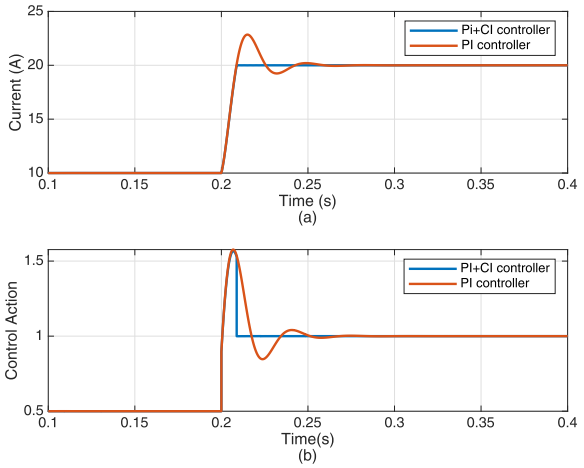

FIGURE 11. A comparison in simulation of (a) step response of the linear PI and the reset $PI + CI$ controllers showing the flat response that can be achieved and (b) the control action.

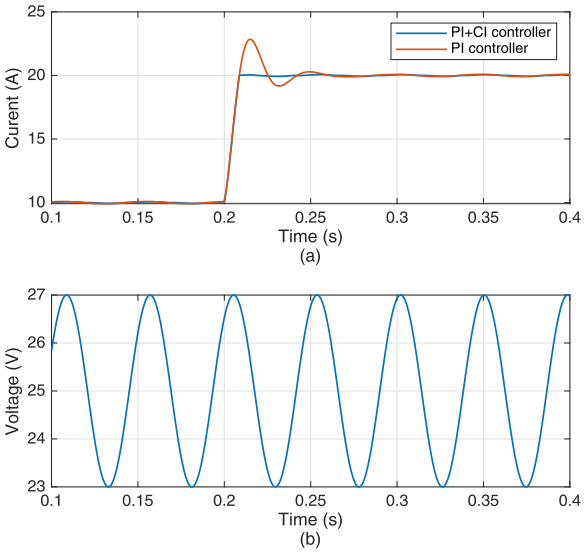

FIGURE 12. Step response of the controller under a varying input voltage (a) Step response comparison between PI and $PI + CI$ controller (b) varying input voltage.

$PI + CI$ controllers when subjected to a step change in reference value from 10A to 20 A. The ability of reset controller in improving the tracking performance is clearly observable by the flat response that it produces in Fig.11(a). The maximum overshoot with PI controller is around 22.8 A and this was eliminated by the PI+CI controller which resulted in 12 % reduction in overshoot.

The control action generated by the PI and PI+CI controller is shown in Fig.11(b). The reset action of the integrator state at the instance of zero crossing is clearly visible here. This also gives an understanding of how the reset controller achieves the flat response. It can be observed from Fig.11(b) that with classical PI controller the integrator state, after the first zero crossing, takes a finite amount of time to reach its steady state value which ultimately leads to large overshoot and oscillatory response. In the PI+CI controller based system this is avoided through reset action, which forces the integrator to its steady state value at first zero crossing. The utilisation of reset ratio ρ_r obtained from (16) ensures that integrator output is driven to its steady state value.

The DC-DC boost converter, in the application considered here, is operated as a current source with the objective to deliver a reference value of current at the output. Under this scenario the robustness of PI+CI controller can be ascertained by assessing whether it can ensure a flat response to step change in reference while also being subjected to a varying input voltage. This is highlighted in Fig.12 where the converter step response while also being subjected to a varying input voltage is shown. The input source in grid connected application for DC-DC converter can be renewable sources or storage systems like batteries, fuel cell etc. The voltage variation exhibited by these sources tend to be of lower time constant. In the results shown in Fig.12 this is emulated through a DC voltage source superimposed with a sine wave as shown in Fig.12.(b). The resulting step response is given in Fig.12.(a). It can be seen that the PI+CI controller is still capable of eliminating the overshoot in comparison to PI controller under input voltage variation. It should be noted that in the steady state both controllers exhibit a small oscillatory behaviour due to the input voltage variation. This is to be expected as the PI+CI controller only targets and improves the transient response by eliminating the overshoot and ensuring a fast settling to steady state value. The robustness of controller to measurement noise will be discussed through the experimental results presented in the next section.

B. EXPERIMENTAL IMPLEMENTATION AND RESULTS

The Fig.13 shows the laboratory set up where the proposed $PI + CI$ controller was implemented. The DC-DC converter uses IGBT modules from Semikron. The Höcherl & Hackl NL series programmable source/sink was used as input DC source and DC grid was emulated through the Höcherl & Hackl ZS series electronic load. The controller was implemented in FPGA (CompactRIO from NI) using LabVIEW. Hall sensors were used for output current sensing. The data acquisition to the controller is carried out using NI 9201 C series voltage input modules which captures the hall sensor outputs and samples at 16 μs per channel. The experimental results shown here are based on the output of these modules obtained through LabVIEW interface.

The Fig.14 shows tracking performance of the converter under a varying reference alternating between 10A and 20A when used with PI_{base} (fast PI) controller. The higher overshoot which arises at converter output due the fast PI action from the PI_{base} controller can be noticed in Fig.14 and is emphasised in Fig.15 where the rising edge of the step response is zoomed into. These overshoots when injected into weak grids can cause voltage variations beyond permissible limit. It is this overshoot which can be negated with well designed reset control.

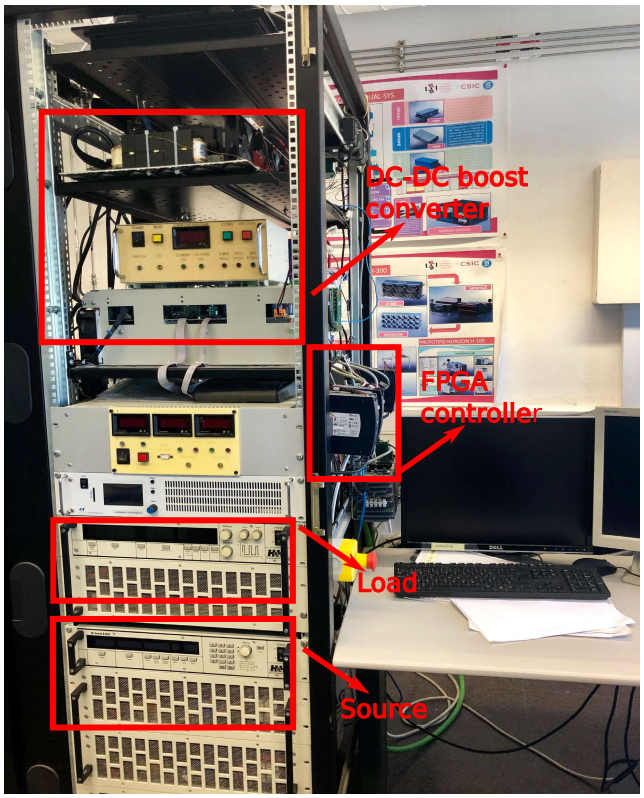

FIGURE 13. Laboratory setup of the DC-DC boost converter with programmable source and sinks.

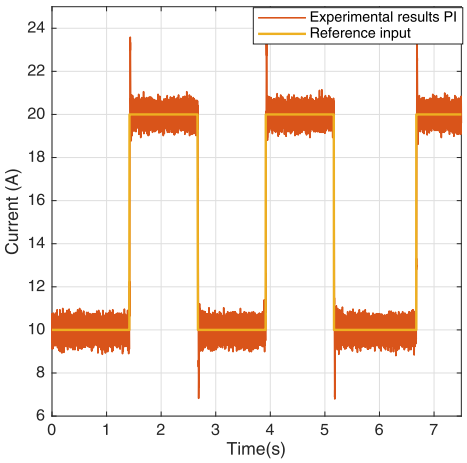

FIGURE 14. Reference tracking performance of the converter (red) when used with PI_{base} controller for reference input (orange). The overshoot with PI_{base} controller can be observed here.

The Fig. 16 shows reference tracking of the converter when using the $PI + CI$ controller under a reference value alternating between 10A and 20A. In comparison to Fig.14 the tracking performance under $PI + CI$ is devoid of overshoots as shown in Fig.16 when subjected to step change in reference value. The absence in overshoot is clearly observed in Fig.17 where the response in Fig.16 is zoomed at a rising edge. The peak value at the transient period for the $PI + CI$

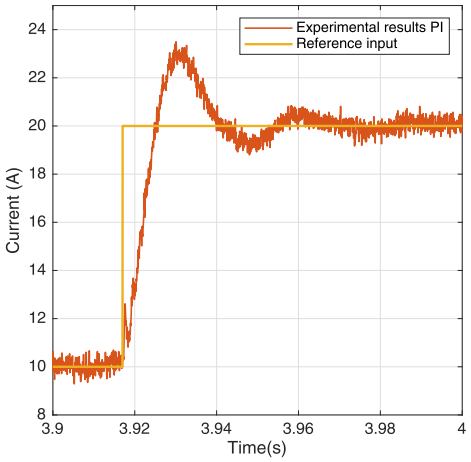

FIGURE 15. Zoom in near a rising edge of the step response in Fig.14 highlighting the overshoot resulting from PI_{base} controller.

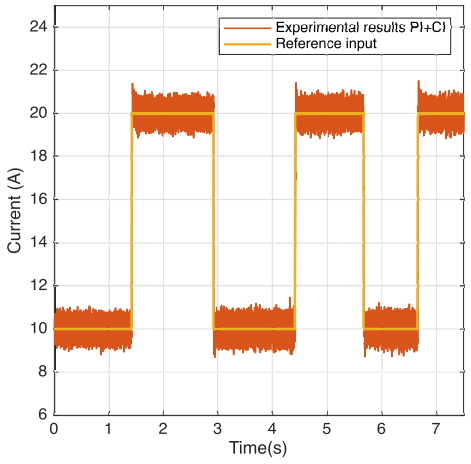

FIGURE 16. Reference tracking performance of converter set up (red) when used with $PI + CI$ reset controller. The flatter response from reset control is observed.

controller based system shows an almost 10 % reduction in overshoot in comparison to that of the PI controller in Fig.15. This is in close accordance with the simulation results presented in Fig.11 where a 12% reduction in peak overshoot was observed. The slight discrepancy in the values between simulation and experimental results arises from the unmodelled dynamics in the form of delays introduced by filters in data acquisition side, A/D converters which where not considered in the simulation models. The Fig.17 also presents reset signals (violet) which resets the CI at the lower portion of figure. It should also be noted the settling time of the response is faster in the $PI + CI$ controller based system in comparison to the linear system as can be seen from Fig.15 and Fig.17. It is observed that the plot of converter response in Fig.14 and Fig.16 when using both PI and $PI + CI$ controller appears noisy. This is contributed mainly by the measurement noise of high bandwidth Hall sensors used in the current measurement. The effect of measurement noise on the reset action is observable in Fig.17 through the

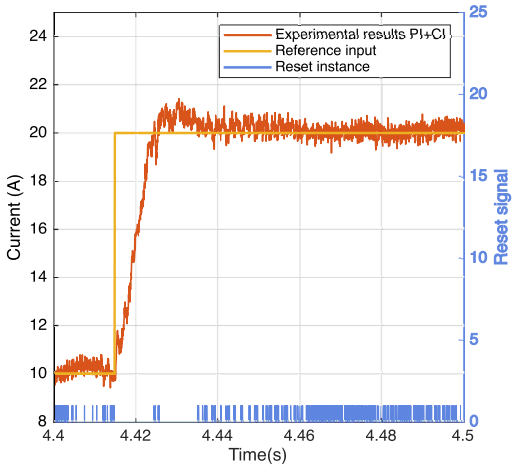

FIGURE 17. Zoom in at rising edge of the step response from Fig.16 emphasizing the flat trajectory achieved with reset control and the reset instances (blue).

reset signals. The noise corrupted signal used in FPGA causes the CI implemented in it to be reset multiple times during steady state condition as evident by the large number of reset signals in Fig.17. Nevertheless it should be noted that the reset signals are well posed (well-defined and are distinct). It should also be noted that the effect of noise inherent to the hall sensor has negligible impact on the stability of the system as evident by the response of PI+CI controller based system in Fig.16 highlighting robustness of the proposed technique under measurement noise. This is also in accordance with the conclusions drawn based on the DF analysis in Section III-B. Based on the analysis it was expected that the PI+CI system be robust to measurement noise.

V. CONCLUSION

The PI+CI controller implemented for the DC-DC boost converter has exhibited improved performance over a well designed PI controller by achieving a flat response. The design of this controller has been relatively straight forward using simple analytical equations and enables easy implementations. In terms of complexity in implementing the same controller in FPGA there is not much increase over the PI_{base} as it simply involves adding an integrator in parallel, which resets at the zero crossings of the error signal. Overall, it can be concluded that the $PI + CI$ reset controller provides better performance without increasing the complexity in terms of design, implementation and sensitivity to sensor noise. These converters, capable of producing flat fast responses can find increased application in grid connected systems to respond to sudden load changes without creating much deviations from the prescribed nominal values.

In terms of future work there are many issues which can be addressed, the most important being the disturbance rejection capabilities of these controllers especially for converters which are employed in hybrid system applications like the electric grids.

REFERENCES

[1] J. Clegg, "A nonlinear integrator for servomechanisms," *Trans. Amer. Inst. Electr. Eng. II, Appl. Ind.*, vol. 77, no. 1, pp. 41–42, Mar. 1958.
[2] K. R. Krishnan and I. M. Horowitz, "Synthesis of a non-linear feedback system with significant plant-ignorance for prescribed system tolerances," *Int. J. Control*, vol. 19, no. 4, pp. 689–706, Apr. 1974.
[3] I. Horowitz and P. Rosenbaum, "Non-linear design for cost of feedback reduction in systems with large parameter uncertainty," *Int. J. Control*, vol. 21, no. 6, pp. 977–1001, 1975.
[4] L. Zaccarian, D. Nešić, and A. R. Teel, "Analytical and numerical Lyapunov functions for SISO linear control systems with first-order reset elements," *Int. J. Robust Nonlinear Control*, vol. 21, no. 10, pp. 1134–1158, 2011.
[5] L. Zaccarian, D. Nesic, and A. R. Teel, "First order reset elements and the clegg integrator revisited," in *Proc. Amer. Control Conf.*, vol. 1, Jun. 2005, pp. 563–568.
[6] D. Nesic, A. R. Teel, and L. Zaccarian, "Stability and performance of SISO control systems with first-order reset elements," *IEEE Trans. Autom. Control*, vol. 56, no. 11, pp. 2567–2582, Nov. 2011.
[7] A. Banos and A. Barreiro, "Delay-independent stability of reset systems," *IEEE Trans. Autom. Control*, vol. 54, no. 2, pp. 341–346, Feb. 2009.
[8] A. Baños and A. Vidal, "Design of reset control systems: The PI+CI compensator," *J. Dyn. Syst., Meas., Control*, vol. 134, no. 5, 2012, Art. no. 051003.
[9] A. Baños and M. Davó, "Tuning of reset proportional integral compensators with a variable reset ratio and reset band," *IET Control Theory Appl.*, vol. 8, no. 17, pp. 1949–1962, 2014.
[10] O. Beker, C. V. Hollot, and Y. Chait, "Plant with integrator: An example of reset control overcoming limitations of linear feedback," *IEEE Trans. Autom. Control*, vol. 46, no. 11, pp. 1797–1799, Nov. 2001.
[11] A. Baños and A. Barreiro, *Reset Control Systems*. Springer, 2011.
[12] A. Ba nos, J. I. Mulero, A. Barreiro, and M. A. Davó, "An impulsive dynamical systems framework for reset control systems," *Int. J. Control*, vol. 89, no. 10, pp. 1985–2007, 2016.
[13] J. Carrasco, A. Baños, and A. van der Schaft, "A passivity-based approach to reset control systems stability," *Syst. Control Lett.*, vol. 59, no. 1, pp. 18–24, Jan. 2010.
[14] A. F. Villaverde, A. B. Blas, J. Carrasco, and A. B. Torrico, "Reset control for passive bilateral teleoperation," *IEEE Trans. Ind. Electron.*, vol. 58, no. 7, pp. 3037–3045, Jul. 2011.
[15] A. Vidal, A. Baños, J. C. Moreno, and M. Berenguel, "PI+CI compensation with variable reset: Application on solar collector fields," in *Proc. IEEE 34th Annu. Conf. Ind. Electron.*, Nov. 2008, pp. 321–326.
[16] M. F. Heertjes, K. G. J. Gruntjens, S. J. L. M. van Loon, N. van de Wouw, and W. P. M. H. Heemels, "Experimental evaluation of reset control for improved stage performance," *IFAC-PapersOnLine*, vol. 49, no. 13, pp. 93–98, 2016.
[17] A. Vidal and A. Baños, "Reset compensation for temperature control: Experimental application on heat exchangers," *Chem. Eng. J.*, vol. 159, nos. 1–3, pp. 170–181, May 2010.
[18] J. M. Carrasco, L. G. Franquelo, J. T. Bialasiewicz, E. Galván, R. C. P. Guisado, M. de los Ángeles Martín Prats, J. I. León, and N. Moreno-Alfonso, "Power-electronic systems for the grid integration of renewable energy sources: A survey," *IEEE Trans. Ind. Electron.*, vol. 53, no. 4, pp. 1002–1016, Jun. 2006.
[19] B.-R. Lin and Y.-C. Huang, "Bidirectional DC converter with frequency control: Analysis and implementation," *Energies*, vol. 11, no. 9, p. 2450, 2018.
[20] H. B. Prevez, H. M. García, L. V. Seisdedos, F. C. Muman, and L. A. E. Garcia, "Comparación entre rectificador trifásico con conmutación simétrica y convertidor AC/AC para la mejora del factor de potencia en microcentrales hidroeléctricas," *Revista Iberoamericana Automática Informática Ind.*, vol. 15, no. 1, pp. 101–111, 2017.
[21] K. C. Divya and J. Østergaard, "Battery energy storage technology for power systems—An overview," *Electr. Power Syst. Res.*, vol. 79, no. 4, pp. 511–520, 2009.
[22] P. Denholm, E. Ela, B. Kirby, and M. Milligan, "The role of energy storage with renewable electricity generation," Nat. Renew. Energy Lab., Golden, CO, USA, Tech. Rep. NREL/TP-6A2-47187, 2010.
[23] R. W. Erickson, *Fundamentals of Power Electronics*. Norwell, MA, USA: Kluwer, 2002.
[24] R. S. Ashok and Y. B. Shtessel, "Sliding mode control of electric power system comprised of fuel cell and multiple-modular DC-DC boost converters," in *Proc. 13th Int. Workshop Variable Struct. Syst. (VSS)*, Jun./Jul. 2014, pp. 1–7.

[25] R. S. Ashok, Y. B. Shtessel, and J. E. Smith, "Sliding mode control of electric power system comprised of fuel cells, DC-DC boost converters and ultracapacitors," in *Proc. Amer. Control Conf.*, Jun. 2013, pp. 5766–5771.
[26] V. Ramanarayanan, "Sliding mode control of power converters," Ph.D. dissertation, Dept. Eng. Appl. Sci., California Inst. Technol., Pasadena, CA, USA, 1986.
[27] P. Thounthong, P. Tricoli, and B. Davat, "Performance investigation of linear and nonlinear controls for a fuel cell/supercapacitor hybrid power plant," *Int. J. Elect. Power Energy Syst.*, vol. 54, pp. 454–464, Jan. 2014.
[28] U. R. Nair and R. Costa-Castelló, and A. Baños, "Reset control of boost converters," in *Proc. IEEE Annu. Amer. Control Conf. (ACC)*, Jul. 2018, pp. 553–558.
[29] O. Beker, C. Hollot, Y. Chait, and H. Han, "Fundamental properties of reset control systems," *Automatica*, vol. 40, no. 6, pp. 905–915, Jun. 2004.
[30] R. Goebel, R. G. Sanfelice, and A. R. Teel, *Hybrid Dynamical Systems: Modeling, Stability, and Robustness*. Princeton, NJ, USA: Princeton Univ. Press, 2012.
[31] S. J. L. M. Van Loon, K. G. J. Gruntjens, M. F. Heertjes, N. Van de Wouw, and W. P. M. H. Heemels, "Frequency-domain tools for stability analysis of reset control systems," *Automatica*, vol. 82, pp. 101–108, Aug. 2017.
[32] F. Guinjoan, J. Calvente, A. Poveda, and L. Martinez, "Large-signal modeling and simulation of switching DC-DC converters," *IEEE Trans. Power Electron.*, vol. 12, no. 3, pp. 485–494, May 1997.
[33] P. Chrin and C. Bunlaksananusorn, "Large-signal average modeling and simulation of DC-DC converters with SIMULINK," in *Proc. IEEE Power Convers. Conf. Nagoya*, Apr. 2007, pp. 27–32.
[34] T. Hägglund and K. J. Åström, "Revisiting the Ziegler-Nichols tuning rules for Pi control," *Asian J. Control*, vol. 4, no. 4, pp. 364–380, 2002.
[35] A. R. Bergen and R. L. Franks, "Justification of the describing function method," *SIAM J. Control*, vol. 9, no. 4, pp. 568–589, 1971.
[36] A. Mees and A. R. Bergen, "Describing functions revisited," *IEEE Trans. Autom. Control*, vol. AC-20, no. 4, pp. 473–478, Aug. 1975.
[37] S. R. Sanders, "On limit cycles and the describing function method in periodically switched circuits," *IEEE Trans. Circuits Syst. I, Fundam. Theory Appl.*, vol. 40, no. 9, pp. 564–572, Sep. 1993.
[38] K. J. Aström and R. M. Murray, *Feedback Systems: An Introduction for Scientists and Engineers*. Princeton, NJ, USA: Princeton Univ. Press, 2010.

UNNIKRISHNAN RAVEENDRAN NAIR was born in Thiruvananthapuram, India, in 1989. He received the B.Tech. degree from Kerala University, India, in 2011, and the masters' degree in CIVILINGENIØR I ENERGITEKNIK from Aalborg University, Denmark, in 2015. He is currently pursuing the Ph.D. degree with the Universitat Politècnica de Catalunya, Spain, as a Marie Curie Research Fellow. From 2015 to 2016, he was with the Energy Technology Department, Aalborg University, where he pursued research on developing high frequency SiC power modules, packaging techniques for SiC MOSFETs, and the design of RF power converters. His current research interests include the control and management of energy storage system in microgrid with focus on robust, predictive control, and forecasting techniques.

RAMON COSTA-CASTELLÓ was born in Lleida, Spain, in 1970. He received the B.S. and Ph.D. degrees in computer science from the Universitat Politècnica de Catalunya (UPC), Spain, in 1993 and 2001, respectively, where he is currently an Associate Professor with the Automatic Control Department. His teaching activity is related to different aspects in automatic control. His research is focused on the analysis and development of energy-management systems (automotive and stationary applications) and the development of digital control techniques. He is a member of the Spanish Association of Automatic Control (CEA), IFAC EDCOM Technical Committee 9.4 Member, the Automotive Control Technical Committee 7.1 Member, and the IEEE Senior Member of the Control System Society.

ALFONSO BAÑOS was born in Córdoba, Spain, in 1965. He received the Licenciado and Ph.D. degrees in physics from the Complutense University of Madrid, in1987 and 1991, respectively. From 1988 to 1992, he was with the Instituto de Automática Industrial (CSIC), Madrid, where he pursued research in nonlinear control and robotics. In 1992, he joined the Universidad de Murcia, where he is currently a Professor in automatic control. He has also held visiting appointments at the University of Strathclyde, the University of Minnesota at Minneapolis, and the University of California at Berkeley. His research interests include robust and nonlinear control and reset/hybrid control, with applications in process control and networked control systems.